Published in final edited form as:
J Immunol. 2012 November 1; 189(9): 4295–4304. doi:10.4049/jimmunol.1200086.

Mouse CD11b+Gr-1+ myeloid cells can promote T helper 17 cell differentiation and experimental autoimmune encephalomyelitis¶

Huanfa Yi[1,2,3,*], **Chunqing Guo**[1,2,3,*], **Xiaofei Yu**[1,2,3], **Daming Zuo**[1,2,3], and **Xiang-Yang Wang**[1,2,3]

[1]Department of Human and Molecular Genetics, Virginia Commonwealth University School of Medicine, Richmond, VA23298, USA

[2]VCU Institute of Molecular Medicine, Virginia Commonwealth University School of Medicine, Richmond, VA23298, USA

[3]VCU Massey Cancer Center, Virginia Commonwealth University School of Medicine, Richmond, VA23298, USA

Abstract

Myeloid-derived suppressive cells (MDSCs) have been a focus of recent study on tumor-mediated immune suppression. However, its role in type 17 helper T (Th17) cell differentiation and the pathogenesis of autoimmune diseases (e.g., multiple sclerosis) has not been determined. We show here that development of experimental autoimmune encephalomyelitis (EAE) in mice is associated with a profound expansion of $CD11b^+Gr\text{-}1^+$ MDSCs, which display efficient T cell inhibitory functions *in vitro*. Unexpectedly, these MDSCs enhance the differentiation of naïve $CD4^+$ T cell precursors into Th17 cells in a highly efficient manner under Th17 polarizing conditions, as indicated by significantly increased number of Th17 cell, elevation of IL-17A production, and upregulation of the orphan nuclear receptor RORA and RORC. Mechanistic studies show that IL-1β represents a major mediator of MDSC-facilitated Th17 differentiation, which depends on the IL-1 receptor on $CD4^+$ T cells but not MDSCs. Selective depletion of MDSCs using gemcitabine results in a marked reduction in the severity of EAE (e.g., decreased clinical scores and myelin injury), which correlates with reduced Th17 cells and inflammatory cytokines (IL-17A and IL-1β) in the lymphoid tissues and spinal cords. Adoptively transfer of MDSCs after gemcitabine treatment restores EAE disease progression. Together, we demonstrate for the first time that excessive and prolonged presence of MDSCs can drive a Th17 response and consequently contributes to the pathogenesis of EAE. These new findings provide unique insights into the pleiotropic functions of MDSCs, and may help explain the failure of immunosuppressive MDSCs to control Th17/IL-17-dependent autoimmune disorders.

Keywords

T helper 17 cell; Myeloid-derived suppressor cells; Interleukin-1; multiple sclerosis

¶The present study was supported in part by NIH Grants CA129111 and CA154708; Research Scholar Grant RSG-08-187-01 from American Cancer Society (X.Y.W.). Flow cytometry facility was supported in part by NCI Cancer Center Support Grant to VCU Massey Cancer Center P30CA16059. X.Y.W. is the Harrison Endowed Scholar in the Massey Cancer Center.

Correspondence: Xiang-Yang Wang, Department of Human & Molecular Genetics, PO Box 980033, Virginia Commonwealth University School of Medicine, Richmond, VA 23298. Tel: (804) 628-2679; xywang@vcu.edu.
*Equal contributions

INTRODUCTION

$CD4^+$ T cells play a pivotal role in regulation of the immune response through induction of key cytokines and can differentiate into several subpopulations depending on the stimuli in their environment. The type 17 helper T (Th17) cells are a newly identified inflammatory $CD4^+$ T helper cell subset that is characterized by the production of signature cytokine interleukin (IL)-17 (1, 2). Differentiation of mouse Th17 cells from naïve $CD4^+$ T cells *in vitro* requires CD3 and CD28-mediated stimulation in the presence of IL-6 or IL-21 and transforming growth factor-β (TGF-β) (3). IL-6 and TGF-β are also required for human Th17 cell generation from naïve $CD4^+$ T cells (3–7). Recent studies showed that IL-1β is essential in the early differentiation of both human and mouse Th17 cells as well as conversion of $Foxp3^+$ T cells into IL-17-producing cells (8, 9). Emerging evidence indicates that Th17 cells and IL-17 are associated with pathogenesis of human autoimmune diseases, including multiple sclerosis (MS), rheumatoid arthritis (RA), inflammatory bowel disease, and psoriasis (10).

Myeloid-derived suppressor cells (MDSCs) have become the focus of intense study for the past few years in the context of cancer (11, 12). MDSCs were originally described as a heterogeneous population of immature cells derived from myeloid progenitors with immune-suppressive functions in tumor-bearing hosts. The immune suppressive activity of MDSCs is highly pleiotropic and has been shown to involve a variety of mechanisms (13). In mice, MDSCs are broadly characterized as $CD11b^+Gr\text{-}1^+$ cells, although there are functionally distinct subsets within this population (14, 15). Human MDSCs have been identified as $Lin^-HLA\text{-}DR^{low/-}CD33^+$ (16) or $CD11b^+CD14^-CD33^+$ (17). It has been reported that MDSCs can convert naïve $CD4^+$ T cells *ex vivo* into $Foxp3^+$-expressing regulatory T (Treg) cells (18, 19). The functional importance of MDSCs in the attenuation of immune responses during cancer progression has been documented (13, 20). In addition to cancer, expansion of MDSCs occurs during mycobacteria-induced infection (21) and a mouse model of multiple sclerosis (22), implicating its potential regulatory role under inflammatory conditions. However, their specific contribution to the pathological processes associated with inflammatory autoimmune abnormalities remains to be elucidated.

Although MDSCs and Th17 cells represent two major inflammatory cells often seen under conditions associated with inflammation, functional connection between these two cell populations has not been examined. Experimental autoimmune encephalomyelitis (EAE) represents a well characterized mouse model of human MS, which is induced by immunization of mice with encephalitogenic myelin antigens, i.e., myelin oligodendrocyte glycoprotein (MOG) in the presence of adjuvants (23). The critical roles of Th17 cells and IL-17 in the pathogenesis of this chronic inflammatory disease of the central nervous system have been well documented (24–26). In this report, we show that progression of EAE in mice correlates with concomitant expansion of Th17 cells and MDSCs. We discover that MDSCs can promote Th17 differentiation and IL-17A production highly efficiently under Th17 polarizing conditions in an IL-1β-dependent fashion. We provide the first evidence that depletion of MDSCs with gemcitabine (GEM) markedly reduces the levels of Th17 cell population *in vivo*, and ameliorates the severity of EAE. Furthermore, adoptively transfer of MDSCs to the GEM-treated mice facilitates EAE disease progression, which requires MDSC-derived IL-1β production. Our data establish an important role of MDSCs in modulating development of a Th17 response in mice during chronic inflammation, and suggest that this cell population may serve as a unique target for Th17 cell/IL-17-mediated immunopathology.

MATERIALS AND METHODS

Mice

C57BL/6 mice were obtained from National Cancer Institute (Bethesda, MD). IL-1R1 knockout mice (*il1r1*$^{-/-}$) and B6129F2 mice were obtained from The Jackson Laboratory (Bar Harbor, ME). All experiments and procedures involving mice were approved by the Institutional Animal Care and Use Committee of Virginia Commonwealth University.

Antibodies and reagents

Fluorochrome-conjugated mouse monoclonal antibodies (mAbs), including FITC-CD4 (GK1.5), PE-CD11b (M1/70), PE/Cy5-Gr-1 (RB6-8C5), PE-Foxp3 (MF-14), PE-IFN-γ (XMG1.2) and Percp/Cy5.5-IL-17A (TC11-18H10.1), as well as CD16/CD32 (2.4G2), isotype control rat IgG2b (RTK4530) and IgG1 (RTK2071) were purchased from BioLegend (San Diego, CA). Mouse IL-17A and IL-2 ELISA kits were purchased from BioLegend. PE-conjugated anti-RORγ(t) (AFKJS-9) Abs, mouse IFN-γ and IL-1β ELISA kits were from eBioscience (San Diego, CA). Alexa594-labeled donkey anti-rat secondary IgG was purchased from Invitrogen (Carlsbad, CA). Rat anti-mouse purified anti-CD11b and biotin-conjugated anti-Gr-1 mAbs for immunofluorescence staining were purchased from BD Biosciences (San Diego, CA).

EAE induction and assessment

Mice were immunized subcutaneously at the dorsal flanks with 200 μg $MOG_{35–55}$ peptide (ProSpec Inc., East Brunswick, NJ) emulsified 1:1 in complete Freud's adjuvant (CFA) supplemented with 4 mg/ml heat-killed *Mycobacterium tuberculosis* H37RA (Difco laboratories, Detroit, MI) on day 0. The mice received 200 ng Pertussis toxin (Sigma-Aldrich, St. Louis, MO) intraperitoneally (i.p.) on days 0 and 2. Following the first immunization, the severity of EAE was monitored and graded in a blinded fashion on a scale of 0–5: 0, no disease; 0.5, decreased tail tone; 1, complete limp tail paralysis (flaccid tail); 2, limp tail and one hind limb paralysis; 3, both hind limb paralysis; 4, complete hind limb paralysis and forelimb weakness; 5, morbidity state. Disease incidence and scores were measured daily. For GEM treatment, 8 mg/ml GEM (LC laboratories, Woburn, MA) was injected *i.p.* at 100 mg/kg to EAE mice on days 4, 8, 12, 16 after $MOG_{35–55}$ immunization. Serum was collected 10 days after immunization, and spinal cord (SC) samples were collected 23 days after EAE induction for analysis.

Histology and immunofluorescence

Following an initial perfusion with ice-cold PBS, mice were perfused transcardially with 4% paraformaldehyde and spinal cords with vertebrae were removed. Paraffin-embedded sagittal sections of cervicothoracic spinal cord were stained with Hematoxylin and eosin (H&E) and examined for cellular infiltration or Luxol Fast Blue/Periodic Acid Schiff for determining demyelination. For immunofluorescence, after deparaffinizing in xylene (2×5 min), hydrating with 100% ethanol (2×3 min), 95% ethanol (1 min) and 70% ethanol (1 min) and rinsing in distilled water, paraffin sections (5 μM) of spinal cord were equilibrated in citrate buffer (10 mM, pH 6.0) for 3 min then boiled for antigen retrieval for 10 min in microwave oven, cooled to room temperature (RT), and then rinsed with PBS-Tween 20. After serum blocking for 60 min, the sections were stained with primary mAbs for Gr-1 (1:10), CD4 (1:100) and IL-1β (1:50) and IL-17A (1:50) overnight at 4 °C, followed by incubation with Alexa594-labeled donkey anti-rat secondary IgG at RT for 1 hour. A negative staining control was performed by incubation with isotype control Abs. The coverslips were mounted using Vectashield mounting medium (Vector Labteratories, Inc.

Burlingame, CA) and images were taken using an Olympus BX41 fluorescence microscope (Tokyo, Japan).

Flow cytometry analysis

For surface staining, splenocytes, lymph node cells or mononuclear cells from spinal cord were prepared as single cell suspensions. Cells re-suspended in FACS buffer (PBS containing 0.1% BSA and 0.04% EDTA-Na_2) were blocked with anti-mouse CD16/CD32 mAb (2.4G2, BD Biosciences) and then incubated on ice for 30 minutes with fluorochrome-conjugated Abs or the appropriate isotype controls. For intracellular cytokine staining, cells were stimulated with $MOG_{35–55}$ (1 μg/ml) overnight at 37 °C, 5% CO_2, and treated with phorbol 12-myristate 13-acetate (PMA, 10 nM, Sigma-Aldrich) plus ionomycin (1 μM, EMD Biosciences Inc.) for 5 hours. Brefeldin A (BFA, BioLegend) was added for the last 3 hours of culture. After surface staining with FITC-conjugated anti-CD4 mAbs for 30 min at 4 °C, cells were fixed, permeabilized, and stained with Percp/Cy5.5-conjugated anti-IL-17A, or PE-conjugated anti-IFN-γ or PE-conjugated anti-RORγt mAbs for 30 min at 4 °C. Foxp3 staining was performed according to manufacturer's instruction. For intracellular IL-1β staining, splenocytes were cultured at 37 °C, 5% CO_2 in the presence of BFA for 4 hours. After surface staining with FITC-conjugated CD11b and PE/Cy5-conjugated Gr-1 mAbs for 30 min at 4 °C, cells were fixed, permeabilized, and stained with APC-conjugated IL-1β mAbs for 30 min at 4 °C. Data were then acquired using BD FACSCalibur and analyzed using Flowjo software (Tree Star, Inc., Ashland, OR).

Isolation of mononuclear cells from spinal cords

Mice were perfused with 25 ml ice-cold PBS containing 2 mM EDTA and two intact spinal cords per group were pooled. The SCs were cut into several small pieces and homogenized with Dounce glass homogenizer in 3 ml 1×HBSS. Cell suspension were collected after filtration through 80 μm mesh, and subjected to Percoll gradient (70%/30%) centrifugation (500×g) at 18 °C for 30 min. Mononuclear cells were collected from the 30%/70% interface and washed, re-suspended in FACS buffer or T cell medium and used for subsequent experiments.

Isolation of MDSCs and subsets

Spleen-derived MDSCs were purified from EAE mice using $CD11b^+$ magnetic beads (Miltenyi Biotec, Auburn, CA). Approximately 98% of $CD11b^+$ cells are $Gr\text{-}1^+$ and the purity of $CD11b^+$ $Gr\text{-}1^+$ cells were typically greater than 95%. In some experiments, $CD11b^+Gr\text{-}1^+$were sorted from splenocytes and $CD11b^+Gr\text{-}1^{low}$ and $CD11b^+Gr\text{-}1^{high}$ cells were sorted from bone marrow using the BD Biosciences FACSAria II cell sorter (San Jose, CA).

Immunosuppression assays by MDSCs and cytokine detection

Control splenocytes (2×10^5 cells/well) were cocultured with purified MDSCs at different ratios as indicated in the figures, in the presence of 1 μg/ml plate-bound anti-CD3 mAb (145–2C11, BioXcell, Inc. West Lebanon, NH) and 0.5 μg/ml soluble anti-CD28 mAb (37.51, BioLegend Inc. San Diego, CA) in 96-well flat-bottom plate for 72 hours. Cells were pulsed with 0.5 μCi/well ^{3}H-thymidine for the last 16 hours of incubation. Proliferation was measured by mean^{3}H-thymidine incorporation in triplicate wells using a LS 6500 multi-purpose scintillation counter (Beckman Coulter, USA). Supernatant was collected 48 hours after culture, levels of cytokines IL-2 and IFN-γ were determined by ELISA according to the manufacturer's instructions.

In vitro Th17 cell differentiation

$CD4^+CD25^-CD62L^{high}$ naïve T cells were FACS sorted (> 98% pure) and 5×10^5/well cells were activated with plate-bound 5 μg/ml anti-CD3 plus 1 μg/ml soluble anti-CD28 Abs in the presence of 2.5 ng/ml hTGF-β (Peprotech, Rocky Hill, NJ), 20 ng/ml mIL-6 (Peprotech), 5 μg/ml anti-IFN-γ (XMG1.2, BioXcell) and anti-IL-4 (11B11, Biolegend) mAbs in 24-well plates. MDSCs were added to the culture on day 0 at a ratio of 1:1 (MDSC: T cell). Cells were cultured in triplicate in RPMI media supplemented with 10% FCS, 50 μM β-mercaptoethanol, 2 mM L-glutamine/1% penicillin/streptomycin. 3 days after activation, supernatants were collected for IL-17A or IL-1β cytokine assays by ELISA according to manufacturer's instructions. Cells were washed and stimulated with PMA plus ionomycin in the presence of Golgi-stop for 4 hours, followed by intracellular staining for IL-17A and IFN-γ-producing $CD4^+$ cells. Intracellular staining for Foxp3 was performed with a Foxp3 staining kit (eBioscience). Cell proliferation was assessed using CFSE dilution assays. In some experiments, 10 ng/ml IL-1β (BioLegend), 30 μg/ml IL-1β mAbs (Biolegend), 200 ng/ml Interleukin-1 receptor antagonist (IL-1ra, ProSpec, Inc.), or 10 μg/ml anti-TGF-β mAbs (Biolegend) were added.

Real-time PCR analysis

Total RNAs were prepared using TRIzol reagent (Invitrogen, Carlsbad, CA) from spleen, lymph nodes, spinal cord or cultured Th17 cells. RNA was treated with RNase-free DNase I (Invitrogene, Carlsbad, CA) to eliminate the contamination of genomic DNA and quantified using an Ultra-Spec spectrophotometer (Amersham Bioscience, Piscataway, NJ). Complementary DNA (cDNA) was synthesized with Revert AidTM MMLV Reverse Transcriptase (Ferments Inc., Glen Burnie, MA) in 20 μl reaction volumes containing 1 μg of total RNA and 50 ng oligo(dT) primers (Invitrogen). For quantitative PCR analysis, transcription profiles of *il17a*, *rora*, *rorc*, *il1b* were assessed on an ABI prism 7900HT Sequence Detection System using TaqMan Universal PCR Master Mix (Applied Biosystems, Foster City, CA). Primers and FAM-labeled probe sets were obtained as pre-developed assay reagents from Applied Biosystems: *il17a*, Mm00439618_m1, *rora*, Mm00443103_m1; *rorc*, Mm01261022_m1; *il1b*, Mm01336189_m1. The PCR was started with 2 min at 50 °C and an initial 15 min denaturation at 94 °C, followed by a total of 40 cycles of 15 sec denaturation at 94 °C, and 1 min of annealing and elongation at 60 °C. All measurements were performed in triplicate wells and repeated three times. Gene expression was quantified relative to the expression of the housekeeping gene *gapdh*, and normalized to that measured in control cells by standard $2^{(-\Delta\Delta CT)}$ calculation.

Adoptive cell transfer

MDSCs-derived from EAE mice were treated with or without caspase-1 inhibitor (Cayman Chemical, 100 μM) prior to adoptive transfer. C57BL/6 mice (n=5) were immunized with $MOG_{35–55}$/CFA, followed by GEM (50 mg/kg) administration after the disease onset twice at 4-day intervals. 4 days after GEM treatment, mice were transferred *i.v.* with MDSCs (8×10^6) twice at one week interval. The progression of EAE disease was followed and clinical scores were recorded.

Statistical analysis

Statistical analysis was performed with Prism Software (GraphPad, San Diego, CA). Data are shown as the mean ± SEM. Unpaired 2-tailed student *t* test was used for two group comparisons. Where there were more than two groups, differences between groups were tested with analysis of variance (ANOVA) test. *p* values less than 0.05 were considered statistically significant.

RESULTS

Expansion of Th17 cells and MDSCs during the EAE progression

Th17 cells play a prominent role in the pathogenesis of autoimmune diseases (e.g., EAE). As expected, a substantial increase of the percentage of IL-17A-producing $CD4^+$ T cells was detected after EAE induction, as indicated by intracellular cytokine staining and flow cytometry analysis of splenocytes in EAE mice (Fig. 1A, upper). Interestingly, the increase in Th17 cells was concomitant with marked expansion of $CD11b^+Gr\text{-}1^+$ myeloid cells in the spleen (Fig. 1A, middle) and peripheral blood (Fig. 1A, lower). The increase of $CD11b^+Gr\text{-}1^+$ cell population in peripheral blood during the disease progression in EAE mice was time-dependent (Fig. 1B).

The phenotype of $CD11b^+Gr\text{-}1^+$ cells expanded during the EAE disease progression is highly similar to previously defined tumor-associated MDSCs. These cells can also be subdivided into two subsets, i.e., $CD11b^+Ly6C^{high}Ly6G^-$ and $CD11b^+Ly6C^{low}Ly6G^+$which correspond to monocytic MDSCs (M-MDSC) and granulocytic MDSCs (G-MDSC), respectively, and both of which expanded during the development of EAE (Supplementary Fig. S1A-B). Phenotypic similarity is also supported by FSC/SSC characteristic and morphology analyses. In contrast to inflammatory monocytes that often express F4/80 and CD80 (27), these myeloid cells do not express these two markers, as well as CD11c and MHCII, which resembles the immature or undifferentiated myeloid cells (Supplementary Fig. S1C). However, they share some phenotypic characteristics with inflammatory monocytes, e.g., expression of CD115, CCR2 and CD62L (Supplementary Fig. S1D).

This $CD11b^+Gr\text{-}1^+$ cell population is also functionally similar to $CD11b^+Gr\text{-}1^+$ MDSCs often seen in cancer-bearing hosts, as evidenced by their highly efficient activity in suppressing the proliferation and cytokine (IFN-γ and IL-2) production of T cells following TCR-engagement or antigen ($MOG_{35–55}$)-specific stimulation (Fig. 1C-E, Supplementary Fig. S1E-G). These results are also consistent with a recent report showing that $CD11b^+Ly6C^+$ cells increased during the inflammatory phase of the EAE and induced potent inhibition of T cell activation (22). Therefore, $CD11b^+Gr\text{-}1^+$ cells (henceforth called MDSCs) that is enriched and accumulated in peripheral lymphoid tissues of the EAE mice may play a regulatory role in development of a Th17 response.

MDSCs promote Th17 cell differentiation under Th17-polorizing conditions

To determine the potential effect of MDSCs on Th17 cell differentiation, we cultured MACS bead-isolated MDSCs with sorted naïve $CD4^+CD25^-CD62L^+$ T cells *ex vivo* for 3 days in Th17 polarizing media, which contained IL-6, TGF-β, anti-IFN-γ and IL-4 mAbs in the presence of plate-bound anti-CD3 mAbs and soluble anti-CD28 mAbs. Strikingly, the presence of MDSCs profoundly increased the percentage of $CD4^+IL\text{-}17A^+$ Th17 cells, but not $CD4^+IFN\text{-}\gamma^+$ Th1 cells or $CD4^+Foxp3^+$ Treg cells (Fig. 2A). The increased percentage of Th17 cells correlated with a significant increase in the expansion of Th17 cells, indicated by CFSE dilution assays and changes of the absolute number of Th17 cells in the culture (Fig. 2B). MDSC-enhanced Th17 polarization was also demonstrated by the elevated protein levels of cytokine IL-17A in the supernatant (Fig. 2C), which correlated with increased the gene transcription of *il17a* and *rora* during Th17 differentiation, indicated by real-time PCR analysis (Fig. 2D). Flow cytometry analysis revealed that the presence of MDSCs also increased the protein levels of RORγt, a key transcription factor that determines the Th17 differentiation (28) (Fig. 2E).

We next assessed the efficiency of MDSCs to promote Th17 polarization by culturing naïve $CD4^+$ T cells with MDSCs at different ratios. MDSCs efficiently enhanced the differentiation of Th17 cells even at a ratio of 1:4, (Fig. 2F). It was found that MDSCs

displayed reduced effectiveness in promoting Th17 cell differentiation when added at the later time points (data not shown), suggesting that the effect of MDSCs mainly occur in the early phase of Th17 cell differentiation. We showed that MDSCs isolated using MACS beads or by cell sorting showed similar activity in driving Th17 cell polarization (Supplemental Fig. S2A). Interestingly, tumor-expanded MDSCs also appeared to efficiently promote Th17 differentiation *in vitro* (Supplementary Fig. S2B). In addition to facilitating Th17 polarization, MDSCs could also enhance the proliferation and IL-17A production of the differentiated Th17 cells (Supplementary Fig. S2C-E).

Considering that MDSCs in mice are broadly grouped into two subpopulations: $CD11b^{+}Gr\text{-}1^{low}$ and $CD11b^{+}Gr\text{-}1^{high}$ that resemble monocytic MDSCs and granulocytic MDSCs, respectively (29, 30), we compared the capacity of these two cell subsets in promoting Th17 cell differentiation. $CD11b^{+}Gr1^{low}$ cells appeared to be much more effective than $CD11b^{+}Gr\text{-}1^{high}$ cells in enhancing Th17 polarization (Fig. 2G).

MDSC-enhanced Th17 differentiation is mediated by IL-1β and requires IL-1 receptor on T cells

We next investigated the potential factors responsible for MDSCs-enhanced Th17 differentiation. IL-6 and TGF-β have been reported as the minimal requirements for murine Th17 cell polarization (31, 32). We initially co-cultured naïve $CD4^{+}$ T cells with MDSCs in the presence of TGF-β plus IL-6, IL-6 alone or TGF-β alone. Lack of exogenous TGF-β disrupted the MDSC-facilitated Th17 differentiation, as indicated by markedly decreased percentage of Th17 cells and IL-17A production (Fig. 3A and 3B, *left*). However, a very low level of Th17 cells and IL-17A could still be detected in the MDSC-T cell culture in the presence of MDSCs (Fig. 3A and 3B, *left*). Use of TGF-βblocking Abs interfered with the effect of MDSCs when only IL-6 was present in the culture (Fig. 3B, *right*). Given the previously documented TGF-β expression by MDSCs (33, 34), MDSCs may be able to partially compensate for the absence of exogenous TGF-β. In sharp contrast, absence of exogenous IL-6 completely abolished Th17 polarization in the presence of MDSCs (Fig. 3A and 3B, *left*), indicating an indispensable role of this cytokine in the Th17 cell lineage commitment.

In light of recent reports of the importance of IL-1 signaling in the early Th17 differentiation (9, 35, 36), we examined the role of IL-1β in the MDSC-enhanced Th17 differentiation. Blockade of IL-1β using neutralizing mAbs markedly reduced the percentage of Th17 cells (Fig. 3C), which was mirrored by a significant decrease in the IL-17A levels in the supernatants (Fig. 3D). The presence of IL-1R antagonist (IL-1RA), the naturally occurring inhibitor of IL-1β also decreased MDSC-induced IL-17A production (Fig. 3E). Indeed, IL-1β levels were significantly higher in the Th17-polarizing culture system containing MDSCs than in the culture without MDSCs (Fig. 3F), indicating that MDSC represents the major source of IL-1β. The expression of IL-1β in MDSCs was also confirmed by intracellular staining assays (Fig. 3F, *insert*).

We next asked whether IL-1 signaling in T cells or MDSCs was required for the enhanced Th17 differentiation. MDSCs were sorted from WT or *il1r1*$^{-/-}$ mice and co-cultured with naïve T cells-derived from WT or *il1r1*$^{-/-}$ mice, respectively. *Il1r1* deficiency in MDSCs had little effect on Th17 polarization. However, lack of *il1r1* in T cells abolished the stimulating effect of MDSCs on Th17 cell differentiation, indicated by the reduced percentage of Th17 cells and production of IL-17A (Fig. 3G, *left* and *right*).

It was recently reported that $CD11b^{+}$ myeloid cells derived from normal mice and EAE mice exhibited suppressive activity *in vitro* (37). We therefore compared the efficiency of these $CD11b^{+}Gr\text{-}1^{+}$ cells to influence Th17 polarization. MDSCs from EAE mice appeared

to be more effective than those from normal mice in stimulating Th17 cell differentiation (Fig. 3H, *left*). Indeed, EAE mice-derived MDSCs expressed higher levels of IL-1β compared with those from normal mice (Fig. 3H, *right*), suggesting that MDSCs may be stimulated by inflammatory signals in EAE mice. Although inducible nitric oxide synthase 2 (NOS2) and arginase 1 are known to mediate the suppressive activity of MDSCs, we showed that inhibition of arginase 1, not NOS2 diminished the Th17-polarizing activity of MDSCs (Supplementary Fig. S3). Interestingly, blocking arginase 1 activity did not appear to alter the expression of IL-1β expression in MDSCs (Supplementary Fig. S3).

Selective depletion of MDSCs reduced Th17 cells in vivo and EAE severity

It has been reported that GEM can specifically reduce the number of MDSCs in tumor-bearing mice with no significant decrease in T cells, NK cells, macrophages or B cells (38–40). To obtain direct evidence that MDSCs exacerbate EAE disease, we administrated GEM to mice after EAE induction. Treatment with GEM at the dose of 100 mg/kg effectively reduced the MDSC population in peripheral blood and spleen (Fig. 4A), but not other immune cell subsets in lymphoid tissues and peripheral blood (Supplementary Fig. S4A-B). C57BL/6 mice developed severe EAE after immunization with $MOG_{35–55}$ and CFA. However, GEM treatment after EAE induction efficiently blocked EAE development in mice compared to PBS treatment (Fig. 4B). GEM administrated at a lower dose (50 mg/kg) was equally effective, as indicated by complete inhibition of EAE incidence. Treatment with GEM at 10 mg/kg was still able to delay the onset and decreased the severity of the disease (Supplementary Fig. S4C-D). The efficiency of GEM in inhibiting the EAE disease correlated with the levels of MDSCs (Supplementary Fig. S4E).

MDSC depletion by GEM resulted in significantly reduced concentrations of IL-17A in the serum (Fig. 4C) and a substantial decrease in the percentage of $MOG_{35–55}$-specific Th17 cells in the lymph nodes and spleen (Fig. 4D and E). Quantitative RT-PCR showed that gene transcription levels of *rora*, *rorc* and *il17a* in the spleen (Fig. 4F, *left*) and lymph nodes (Fig. 4F, *right*) significantly reduced after GEM treatment. In addition, the mRNA levels of *il1b* in the spleen were significantly lower in GEM-treated EAE mice compared with PBS-treated counterparts (Fig. 4G).

Adoptive transfer assays were conducted to further demonstrate the role of MDSCs in the EAE progression *in vivo*. $MOG_{35–55}$/CFA immunized mice were treated with GEM after disease onset, followed by adoptive transfer of EAE-expanded MDSCs. We showed that GEM treatment after disease onset also inhibited the EAE progression efficiently. However, the transfer of MDSCs restored the disease progression (Fig. 5A). The frequency of $MOG_{35–55}$-specific Th17 cells also increased significantly in the spleen (Fig. 5B) and lymph nodes (data not shown) in mice receiving MDSCs compared to those that were not transferred with MDSCs. To block IL-1β production from MDSCs, we pre-treated MDSCs with the caspase-1 inhibitor prior to cell transfer. These MDSCs failed to accelerate the progression of EAE, which correlated with little change of the frequency of Th17 cells in recipient mice (Fig. 5B). Additionally, transfer of MDSCs or MDSCs pre-treated caspase-1 inhibitor did not appear to influence Th1 and Th2 cells in GEM-treated EAE mice (Fig. 5C).

MDSC depletion with GEM reduces inflammatory cellular infiltration in spinal cords

We examined the effect of GEM treatment on the infiltration of immune cells into the spinal cords, which is generally correlated with disease progression in EAE mice. Flow cytometry analysis of the cellular infiltrates from spinal cords showed that GEM treatment resulted in a marked reduction of infiltrating $CD11b^+Gr\text{-}1^+$ MDSCs (Fig. 6A, *upper*), which was associated with a significant decrease in the percentage of IL-17A-producing $CD4^+$ cells (Fig. 6A, *lower*). The decreased Th17 response in GEM–treated EAE mice was also

indicated by the reduced gene expression of *il17a* in the spinal cords, indicated by quantitative RT-PCR (Fig. 6B).

Histologic analysis showed a massive infiltration of mononuclear cells in the spinal cords of PBS-treated EAE mice. In contrast, mononuclear cell infiltrates and inflammatory foci formation were significantly reduced in the white matter (WM) of spinal cords from GEM-treated EAE mice (Fig. 6C), which is consistent with the reduced clinical scores. $MOG_{35–55}$ immunization-induced myelin injury was indicated by reduced Luxol Fast Blue (LFB) staining and development of widespread vacuolation in the WM (Fig. 6D). Surprisingly, GEM administration effectively improved myelination of the spinal cord, as almost no demyelination was observed in the WM of GEM-treated EAE mice (Fig. 6D). The increase in the density and quality of the myelin in the spinal cords following GEM treatment was also associated with significantly reduced levels of inflammatory cell infiltrates (Fig. 6D).

Immunofluorescence staining was used to further examine the infiltration of inflammatory cells in the spinal cords from EAE mice treated with or without GEM. The spinal cord tissues from GEM treated mice showed substantially decreased infiltration $CD4^+Gr\text{-}1^+$ and $IL\text{-}17A^+$ cells compared with PBS-treated EAE mice (Fig. 6E). GEM treatment similarly caused a pronounced reduction in IL-1β-producing cells in the spinal cords of EAE mice (Fig. 6E).

DISCUSSION

Most of the current knowledge regarding the role of MDSCs in immune responses has come from studies in the context of cancer. MDSCs in cancer patients and tumor-bearing mice can subvert immune surveillance by dampening T cell immunity (11, 12). Although expansion of MDSCs has been observed in a mouse model of multiple sclerosis (22), the potential role of the MDSCs in the pathological conditions (e.g., EAE) has not been determined. Our results in this study unveil a complicated inflammatory network in autoimmune disorders, such as EAE. We discover that mouse MDSCs can drive the differentiation of Th17 cells under Th17-polarizing conditions (e.g., in the presence of cytokines IL-6 and TGF-β). Instead of curbing T cell activation or facilitating the resolution of inflammation, the excessive expansion and the prolonged accumulation of MDSCs may have detrimental effect by enhancing development of Th17 cells, which can further drive tissue inflammation and aggravating tissue damage in autoimmune diseases.

We provide here the first evidence that MDSCs stimulate Th17 cell polarization and IL-17A production in a highly efficient manner. This finding is striking, considering the well-established immunosuppressive activity of MDSCs. It should be noted that, while we specifically examine the effect of MDSCs on the expansion of $CD4^+IL\text{-}17^+$ T cells under Th17 polarizing conditions or during the differentiation of naïve T precursor cells, whereas all other reports only examine the immunosuppressive activity of MDSCs on T cells in the context of antigen stimulation or TCR engagement. Together with the previous reports of MDSCs-facilitated conversion of naïve $CD4^+$ T cells into $Foxp3^+$-expressing regulatory T (Treg) cells *ex vivo* (18, 19), our results indicate that MDSCs can display pleiotropic functions under different physiological and pathological conditions, and the pro-Th17 effect of MDSCs may be uncoupled from its T cell suppressive activity. We postulate that the capability of MDSCs to differentially regulate T cell or drive its lineage commitment depends on the inflammatory environment and cytokines existing in the inflamed sites. Our new findings may provide an explanation why MDSCs mobilized under pathological conditions (e.g., EAE) ‘fail’ to materialize their immunosuppressive potential. Instead, these MDSCs can facilitate an inflammatory Th17 response or IL-17A production, and further promote chronic inflammation as well as the pathogenesis of autoimmune diseases.

Therefore, caution should be used in applications of MDSCs for treatment of autoimmune diseases. Our findings also indicate that understanding of action of MDSCs in the host responses and disease progression is far from complete, and future studies should not only investigate the regulatory role of MDSCs in the development as well as activities of T cells of different lineages in different contexts, but also explore other potential effects of MDSCs beyond the established immunosuppressive activity.

Our results from independent systems demonstrate that IL-1β plays an important role in mediating MDSC-stimulated Th17 cell generation. We confirm that IL-1R expression in $CD4^+$ T cells, but not on MDSCs, is needed for MDSC-promoted Th17 cell development. This observation supports the recent finding of Dong and colleagues that IL-1 signaling in T cells was required for early Th17 cell differentiation (9). Interestingly, human myeloid cells (e.g., monocytes) isolated from the site of rheumatoid arthritis were also shown to increase a Th17 response, however, in an IL-1β-independent fashion (41). Although our studies support the notion that IL-1β represents a major factor involved in MDSC-facilitated Th17 polarization, other IL-1β-independent mechanisms underlying this phenomenon remain the possibility, given the plasticity and heterogeneity of this cell population. In the present study, we also observe that arginase 1 is needed for the effect of MDSCs in Th17 differentiation. However, inhibition of arginase 1 activity does not appear to affect IL-1β production from MDSCs, suggesting that MDSCs-associated IL-1β or arginase 1 regulates Th17 polarization *via* independent mechanisms. It is possible that excessive nitric oxide production in the presence of arginase 1 inhibitor (42) may be able to suppress Th17 differentiation, as recently documented by Niedbala *et al* (43). Given the multiple effects of arginase activity and potential different outcomes (42), further studies are necessary to understand the precise role of arginase 1 in MDSC-driven Th17 polarization.

GEM has been used clinically as an approved therapeutic agent, and was recently shown to improve antitumor immune responses by selectively targeting MDSCs in several preclinical models (38–40). Our results demonstrate that MDSC depletion after GEM administration effectively ameliorates the clinical symptoms in EAE mice, which is attributed to significantly reduced levels of IL-17A-producing Th17 cells in peripheral tissues and inflamed disease sites (e.g., spinal cords). Furthermore, adoptively transfer of EAE-expanded MDSCs to GEM-treated mice can restore the EAE disease progression, whereas pre-treatment of MDSCs with caspase-1 inhibitor for blocking IL-1β production disrupts this effect. This result strongly supports the critical role of MDSC-derived IL-1β in enhanced Th17 response and EAE progression *in vivo*. Given the potency of GEM in blockade of MDSC-driven Th17 response, the potential benefits of using this agent for treatment of inflammatory autoimmune diseases (e.g., EAE) warrant further investigation. However, more studies are necessary to define the sensitivity of MDSCs and other cell subsets to the GEM effect.

Recently, Ioannou *et al* showed that $CD11b^+Ly6G^+$ cells (G-MDSCs or a subset of neutrophils) decreased the severity of EAE *via* immune suppression-induced by PD-L1/PD-1 interactions (44). Adoptive cell transfer of G-MDSCs in this study was performed starting 4 days after MOG immunization, whereas transfer of total MDSCs in our study occurred after disease onset. It is possible MDSCs exhibit distinct biological activities depending upon the microenvironment at the different pathological stages of autoimmune diseases. As a result, the disease stage must be taken into consideration when MDSCs are exploited for the disease intervention. Ioannou *et al* also showed that only G-MDSCs expanded during the EAE progression, and was able to ameliorate the disease compared to $CD11b^+Ly6G^-$ cells (presumably M-MDSCs). However, other report (22), and our data from the current study demonstrate that $CD11b^+Ly6C^{high}$ or $CD11b^+Gr\text{-}1^{low}$ cells, mainly comprised M-MDSCs, also expanded in this mouse model of multiple sclerosis. It has been

well documented that M-MDSCs exhibited more potent suppressive activity against T cells compared to $CD11b^{+}Gr\text{-}1^{high}$ cells, represented mostly by G-MDSC (29, 30). Intriguingly, we have shown that $CD11b^{+}Gr\text{-}1^{low}$ cells promote Th17 polarization more efficiently than $CD11b^{+}Gr\text{-}1^{high}$ cells. Therefore, the disparity in these results could be attributed to the plasticity of the phenotype and functions of heterogeneous MDSCs, which may be determined by the environmental or inflammatory milieu.

The present study reveals a previously unknown role of MDSCs during the expansion of Th17 cells and IL-17A production, indicating that the specificity of MDSCs as an immune regulator of T cell differentiation can be dictated by the environment or cytokines present in the inflammatory milieu. Our data demonstrate that MDSCs can contribute to the pathogenesis of autoimmune diseases, e.g., EAE, by promoting Th17 differentiation, and advance our understanding of the biological and pathological roles of MDSCs. These unexpected findings highlight the importance of MDSC-T cell interactions in the shaping of inflammatory T cell responses and suggest that therapeutic targeting of MDSCs may lead to potentially effective intervention of Th17/IL-17-dependent autoimmune disorders.

Supplementary Material

Refer to Web version on PubMed Central for supplementary material.

Abbreviations

Th17	T helper 17 cell
IL-17	Interleukin-17
MDSC	Myeloid-derived suppressor cells
EAE	encephalomyelitis
MOG	myelin oligodendrocyte glycoprotein
MS	multiple sclerosis

REFERENCES

1. Ouyang W, Kolls JK, Zheng Y. The biological functions of T helper 17 cell effector cytokines in inflammation. Immunity. 2008; 28:454–467. [PubMed: 18400188]
2. Korn T, Bettelli E, Oukka M, Kuchroo VK. IL-17 and Th17 Cells. Annu Rev Immunol. 2009; 27:485–517. [PubMed: 19132915]
3. McGeachy MJ, Cua DJ. Th17 cell differentiation: the long and winding road. Immunity. 2008; 28:445–453. [PubMed: 18400187]
4. Wilson NJ, Boniface K, Chan JR, McKenzie BS, Blumenschein WM, Mattson JD, Basham B, Smith K, Chen T, Morel F, Lecron JC, Kastelein RA, Cua DJ, McClanahan TK, Bowman EP, de Waal Malefyt R. Development, cytokine profile and function of human interleukin 17-producing helper T cells. Nat Immunol. 2007; 8:950–957. [PubMed: 17676044]
5. Manel N, Unutmaz D, Littman DR. The differentiation of human T(H)-17 cells requires transforming growth factor-beta and induction of the nuclear receptor RORgammat. Nat Immunol. 2008; 9:641–649. [PubMed: 18454151]
6. O'Garra A, Stockinger B, Veldhoen M. Differentiation of human T(H)-17 cells does require TGF-beta! Nat Immunol. 2008; 9:588–590. [PubMed: 18490908]
7. Yang L, Anderson DE, Baecher-Allan C, Hastings WD, Bettelli E, Oukka M, Kuchroo VK, Hafler DA. IL-21 and TGF-beta are required for differentiation of human T(H)17 cells. Nature. 2008; 454:350–352. [PubMed: 18469800]

8. Acosta-Rodriguez EV, Napolitani G, Lanzavecchia A, Sallusto F. Interleukins 1beta and 6 but not transforming growth factor-beta are essential for the differentiation of interleukin 17-producing human T helper cells. Nat Immunol. 2007; 8:942–949. [PubMed: 17676045]
9. Chung Y, Chang SH, Martinez GJ, Yang XO, Nurieva R, Kang HS, Ma L, Watowich SS, Jetten AM, Tian Q, Dong C. Critical regulation of early Th17 cell differentiation by interleukin-1 signaling. Immunity. 2009; 30:576–587. [PubMed: 19362022]
10. Tesmer LA, Lundy SK, Sarkar S, Fox DA. Th17 cells in human disease. Immunol Rev. 2008; 223:87–113. [PubMed: 18613831]
11. Gabrilovich DI, Nagaraj S. Myeloid-derived suppressor cells as regulators of the immune system. Nat Rev Immunol. 2009; 9:162–174. [PubMed: 19197294]
12. Ostrand-Rosenberg S, Sinha P. Myeloid-derived suppressor cells: linking inflammation and cancer. J Immunol. 2009; 182:4499–4506. [PubMed: 19342621]
13. Marigo I, Dolcetti L, Serafini P, Zanovello P, Bronte V. Tumor-induced tolerance and immune suppression by myeloid derived suppressor cells. Immunol Rev. 2008; 222:162–179. [PubMed: 18364001]
14. Movahedi K, Guilliams M, Van den Bossche J, Van den Bergh R, Gysemans C, Beschin A, De Baetselier P, Van Ginderachter JA. Identification of discrete tumor-induced myeloid-derived suppressor cell subpopulations with distinct T cell-suppressive activity. Blood. 2008; 111:4233–4244. [PubMed: 18272812]
15. Youn JI, Nagaraj S, Collazo M, Gabrilovich DI. Subsets of myeloid-derived suppressor cells in tumor-bearing mice. J Immunol. 2008; 181:5791–5802. [PubMed: 18832739]
16. Kusmartsev S, Su Z, Heiser A, Dannull J, Eruslanov E, Kubler H, Yancey D, Dahm P, Vieweg J. Reversal of myeloid cell-mediated immunosuppression in patients with metastatic renal cell carcinoma. Clin Cancer Res. 2008; 14:8270–8278. [PubMed: 19088044]
17. Liu CY, Wang YM, Wang CL, Feng PH, Ko HW, Liu YH, Wu YC, Chu Y, Chung FT, Kuo CH, Lee KY, Lin SM, Lin HC, Wang CH, Yu CT, Kuo HP. Population alterations of L-arginase- and inducible nitric oxide synthase-expressed CD11b+/CD14/CD15+/CD33+ myeloid-derived suppressor cells and CD8+ T lymphocytes in patients with advanced-stage non-small cell lung cancer. J Cancer Res Clin Oncol. 2009; 136:35–45. [PubMed: 19572148]
18. Huang B, Pan PY, Li Q, Sato AI, Levy DE, Bromberg J, Divino CM, Chen SH. Gr-1+CD115+ immature myeloid suppressor cells mediate the development of tumor-induced T regulatory cells and T-cell anergy in tumor-bearing host. Cancer Res. 2006; 66:1123–1131. [PubMed: 16424049]
19. Hoechst B, Ormandy LA, Ballmaier M, Lehner F, Kruger C, Manns MP, Greten TF, Korangy F. A new population of myeloid-derived suppressor cells in hepatocellular carcinoma patients induces CD4(+)CD25(+)Foxp3(+) T cells. Gastroenterology. 2008; 135:234–243. [PubMed: 18485901]
20. Peranzoni E, Zilio S, Marigo I, Dolcetti L, Zanovello P, Mandruzzato S, Bronte V. Myeloid-derived suppressor cell heterogeneity and subset definition. Curr Opin Immunol. 2010; 22:238–244. [PubMed: 20171075]
21. Dietlin TA, Hofman FM, Lund BT, Gilmore W, Stohlman SA, van der Veen RC. Mycobacteria-induced Gr-1+ subsets from distinct myeloid lineages have opposite effects on T cell expansion. J Leukoc Biol. 2007; 81:1205–1212. [PubMed: 17307863]
22. Zhu B, Bando Y, Xiao S, Yang K, Anderson AC, Kuchroo VK, Khoury SJ. CD11b+Ly-6C(hi) suppressive monocytes in experimental autoimmune encephalomyelitis. J Immunol. 2007; 179:5228–5237. [PubMed: 17911608]
23. Stromnes IM, Goverman JM. Active induction of experimental allergic encephalomyelitis. Nat Protoc. 2006; 1:1810–1819. [PubMed: 17487163]
24. Langrish CL, Chen Y, Blumenschein WM, Mattson J, Basham B, Sedgwick JD, McClanahan T, Kastelein RA, Cua DJ. IL-23 drives a pathogenic T cell population that induces autoimmune inflammation. J Exp Med. 2005; 201:233–240. [PubMed: 15657292]
25. Park H, Li Z, Yang XO, Chang SH, Nurieva R, Wang YH, Wang Y, Hood L, Zhu Z, Tian Q, Dong C. A distinct lineage of CD4 T cells regulates tissue inflammation by producing interleukin 17. Nat Immunol. 2005; 6:1133–1141. [PubMed: 16200068]

26. Komiyama Y, Nakae S, Matsuki T, Nambu A, Ishigame H, Kakuta S, Sudo K, Iwakura Y. IL-17 plays an important role in the development of experimental autoimmune encephalomyelitis. J Immunol. 2006; 177:566–573. [PubMed: 16785554]
27. Geissmann F, Jung S, Littman DR. Blood monocytes consist of two principal subsets with distinct migratory properties. Immunity. 2003; 19:71–82. [PubMed: 12871640]
28. Yang XO, Pappu BP, Nurieva R, Akimzhanov A, Kang HS, Chung Y, Ma L, Shah B, Panopoulos AD, Schluns KS, Watowich SS, Tian Q, Jetten AM, Dong C. T helper 17 lineage differentiation is programmed by orphan nuclear receptors ROR alpha and ROR gamma. Immunity. 2008; 28:29–39. [PubMed: 18164222]
29. Dolcetti L, Peranzoni E, Ugel S, Marigo I, Fernandez Gomez A, Mesa C, Geilich M, Winkels G, Traggiai E, Casati A, Grassi F, Bronte V. Hierarchy of immunosuppressive strength among myeloid-derived suppressor cell subsets is determined by GM-CSF. Eur J Immunol. 2010; 40:22–35. [PubMed: 19941314]
30. Youn JI, Gabrilovich DI. The biology of myeloid-derived suppressor cells: the blessing and the curse of morphological and functional heterogeneity. Eur J Immunol. 2010; 40:2969–2975. [PubMed: 21061430]
31. Bettelli E, Carrier Y, Gao W, Korn T, Strom TB, Oukka M, Weiner HL, Kuchroo VK. Reciprocal developmental pathways for the generation of pathogenic effector TH17 and regulatory T cells. Nature. 2006; 441:235–238. [PubMed: 16648838]
32. Veldhoen M, Hocking RJ, Atkins CJ, Locksley RM, Stockinger B. TGFbeta in the context of an inflammatory cytokine milieu supports de novo differentiation of IL-17-producing T cells. Immunity. 2006; 24:179–189. [PubMed: 16473830]
33. Yang L, Huang J, Ren X, Gorska AE, Chytil A, Aakre M, Carbone DP, Matrisian LM, Richmond A, Lin PC, Moses HL. Abrogation of TGF beta signaling in mammary carcinomas recruits Gr-1+CD11b+ myeloid cells that promote metastasis. Cancer Cell. 2008; 13:23–35. [PubMed: 18167337]
34. Fichtner-Feigl S, Terabe M, Kitani A, Young CA, Fuss I, Geissler EK, Schlitt HJ, Berzofsky JA, Strober W. Restoration of tumor immunosurveillance via targeting of interleukin-13 receptor-alpha 2. Cancer Res. 2008; 68:3467–3475. [PubMed: 18451175]
35. Sutton C, Brereton C, Keogh B, Mills KH, Lavelle EC. A crucial role for interleukin (IL)-1 in the induction of IL-17-producing T cells that mediate autoimmune encephalomyelitis. J Exp Med. 2006; 203:1685–1691. [PubMed: 16818675]
36. Gulen MF, Kang Z, Bulek K, Youzhong W, Kim TW, Chen Y, Altuntas CZ, Sass Bak-Jensen K, McGeachy MJ, Do JS, Xiao H, Delgoffe GM, Min B, Powell JD, Tuohy VK, Cua DJ, Li X. The receptor SIGIRR suppresses Th17 cell proliferation via inhibition of the interleukin-1 receptor pathway and mTOR kinase activation. Immunity. 2010; 32:54–66. [PubMed: 20060329]
37. Slaney CY, Toker A, La Flamme A, Backstrom BT, Harper JL. Naive blood monocytes suppress T-cell function. A possible mechanism for protection from autoimmunity. Immunol Cell Biol. 2011; 89:7–13. [PubMed: 21060323]
38. Suzuki E, Kapoor V, Jassar AS, Kaiser LR, Albelda SM. Gemcitabine Selectively Eliminates Splenic Gr-1+/CD11b+ Myeloid Suppressor Cells in Tumor-Bearing Animals and Enhances Antitumor Immune Activity. Clinical Cancer Research. 2005; 11:6713–6721. [PubMed: 16166452]
39. Le HK, Graham L, Cha E, Morales JK, Manjili MH, Bear HD. Gemcitabine directly inhibits myeloid derived suppressor cells in BALB/c mice bearing 4T1 mammary carcinoma and augments expansion of T cells from tumor-bearing mice. Int Immunopharmacol. 2009; 9:900–909. [PubMed: 19336265]
40. Vincent J, Mignot G, Chalmin F, Ladoire S, Bruchard M, Chevriaux A, Martin F, Apetoh L, Rebe C, Ghiringhelli F. 5-Fluorouracil selectively kills tumor-associated myeloid-derived suppressor cells resulting in enhanced T cell-dependent antitumor immunity. Cancer Res. 2010; 70:3052–3061. [PubMed: 20388795]
41. Evans HG, Gullick NJ, Kelly S, Pitzalis C, Lord GM, Kirkham BW, Taams LS. In vivo activated monocytes from the site of inflammation in humans specifically promote Th17 responses. Proc Natl Acad Sci U S A. 2009; 106:6232–6237. [PubMed: 19325128]

42. Durante W, Johnson FK, Johnson RA. Arginase: a critical regulator of nitric oxide synthesis and vascular function. Clinical and experimental pharmacology & physiology. 2007; 34:906–911. [PubMed: 17645639]

43. Niedbala W, Alves-Filho JC, Fukada SY, Vieira SM, Mitani A, Sonego F, Mirchandani A, Nascimento DC, Cunha FQ, Liew FY. Regulation of type 17 helper T-cell function by nitric oxide during inflammation. Proc Natl Acad Sci U S A. 2011; 108:9220–9225. [PubMed: 21576463]

44. Ioannou M, Alissafi T, Lazaridis I, Deraos G, Matsoukas J, Gravanis A, Mastorodemos V, Plaitakis A, Sharpe A, Boumpas D, Verginis P. Crucial role of granulocytic myeloid-derived suppressor cells in the regulation of central nervous system autoimmune disease. J Immunol. 2012; 188:1136–1146. [PubMed: 22210912]

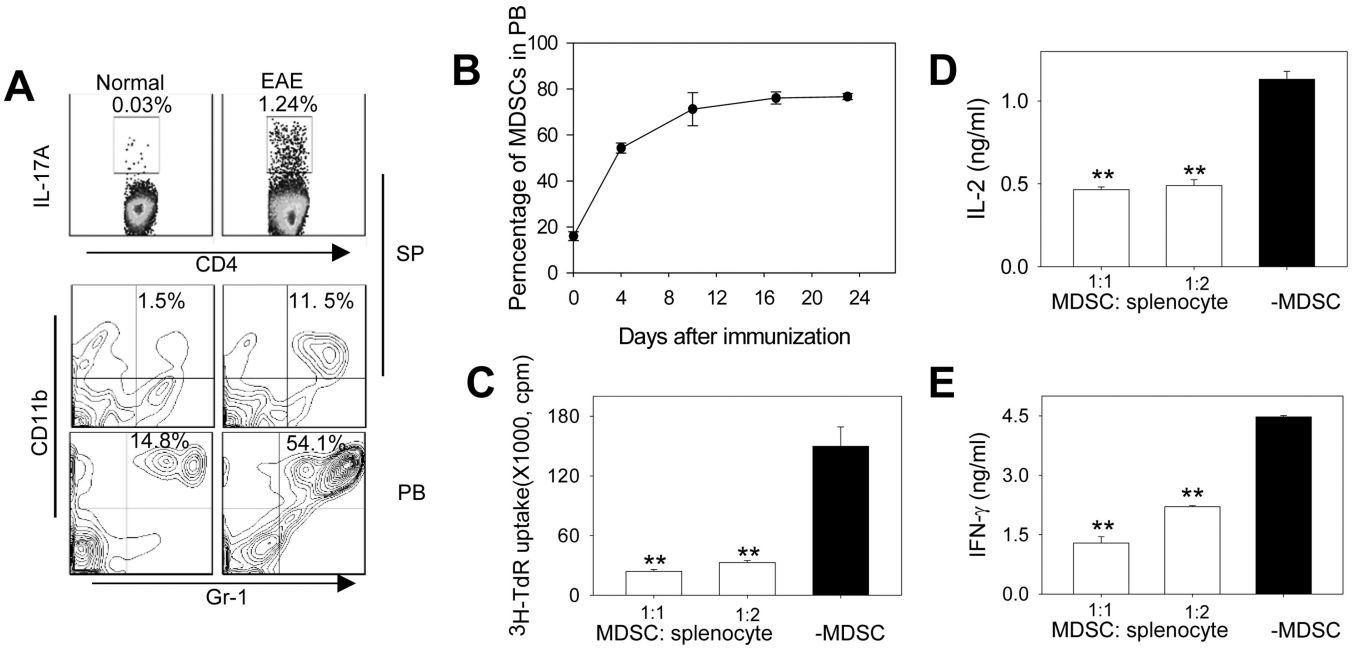

Figure 1. MDSCs profoundly expand during the progression of EAE and display T-cell suppressive activity

A. EAE was induced in C57BL/6 mice (n=5) by immunization with MOG/CFA followed by pertussis toxin injection. The presence of IL-17A-producing $CD4^+$ Th17 cells in the spleen (SP) was examined by flow cytometry 23 days after EAE induction. Percentage of $CD11b^+Gr\text{-}1^+$ MDSCs in the SP and peripheral blood (PB) was also analyzed. The representative histograms from at least three independent experiments with similar results are shown. **B**. Kinetic changes of $CD11b^+Gr\text{-}1^+$ MSDCs during EAE. **C**. MDSCs exhibits immunosuppressive activity against T-cell proliferation. MDSCs were isolated from EAE mice using magnetic beads and co-cultured with splenocytes stimulated with anti-CD3/CD28 mAbs at indicated ratios for 72 hours. Cell proliferation was assessed using ^3H-thymidine (TdR) incorporation assays (**, $p < 0.005$, MDSCs vs no MDSCs).**D and E**. Inhibition of IFN-γ and IL-2 production by MDSCs. After MDSCs co-culture with splenocytes stimulated with anti-CD3/CD28 mAbs, IFN-γ (**D**) and IL-2 (**E**) levels in the culture supernatant were examined using ELISA (**, $p < 0.005$, MDSCs vs no MDSCs). The results represent three independent experiments.

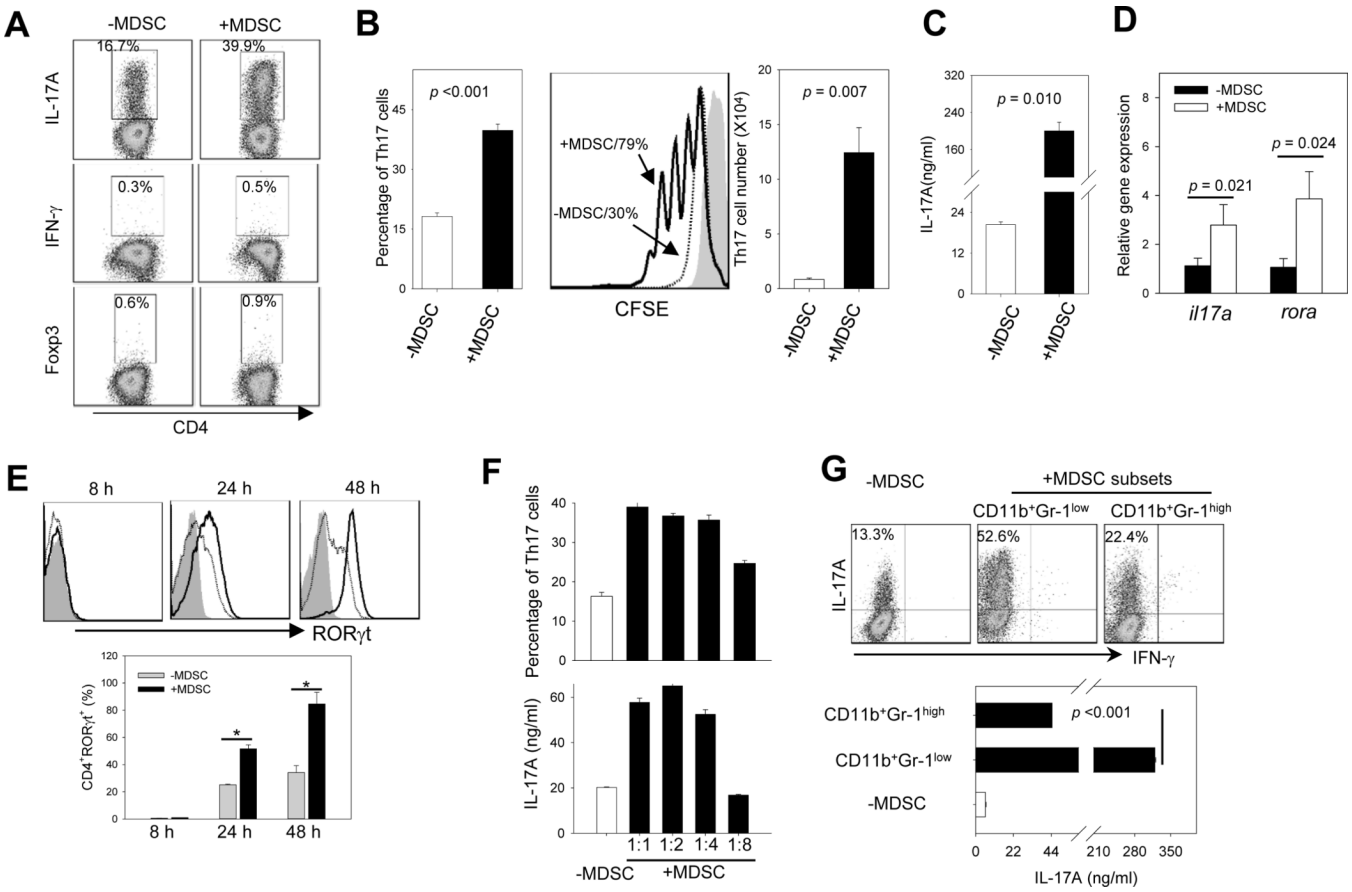

Figure 2. MDSCs are highly efficient in promoting Th17 differentiation in the presence of IL-6 and TGF-β

A. Naïve $CD4^+CD25^-CD62L^+$ T cells (5×10^5 per well in 24-well plates) were co-cultured with or without MDSCs in Th17–polarizing medium for 3 days. Cells were washed and examined for IL-17A or IFN-γ expression by intracellular staining using flow cytometry after stimulation with PMA plus ionomycin in the presence of BFA. $CD4^+Foxp3^+$ cells were also examined by FACS analysis. **B**. The percentage of $CD4^+IL\text{-}17A^+$ T cells (*left*) and total number of $CD4^+IL\text{-}17A^+$ T cells (*right*) after 3-day culture are shown. Cell proliferation in the presence or absence of MDSCs during Th17 cell polarization in the culture was analyzed using CFSE dilution assays (*middle*). **C**. 3 days after co-culture, supernatant was harvested and assessed for IL-17A levels by ELISA. **D**. Relative mRNA levels of *il17a* or *rora* were measured using real-time RT-PCR **E.** RORγt expression during Th17 differentiation was determined using intracellular staining and flow cytometry analysis (*top*, grey filled, isotype control; dashed line, without MDSCs; solid line, with MDSCs). The frequency changes of $CD4^+RORC^+$ T cells in the presence or absence of MDSCs are also shown (*bottom*). **F.** MDSCs were co-cultured with $CD4^+CD25^-CD62L^+$ T cells at different ratios as indicated. The frequency of Th17 cells (*upper*) and IL-17A levels (*lower*) were analyzed. **G.** More efficient Th17 polarization by $CD11b^+Gr\text{-}1^{low}$ MDSCs. $CD11b^+Gr\text{-}1^{low}$ or $CD11b^+Gr\text{-}1^{high}$ cells were cultured with naïve $CD4^+$ T cells. Th17 polarization was examined as described by analyzing the frequency of Th17 cells and IL-17A levels in the culture. The results shown are from three independent experiments.

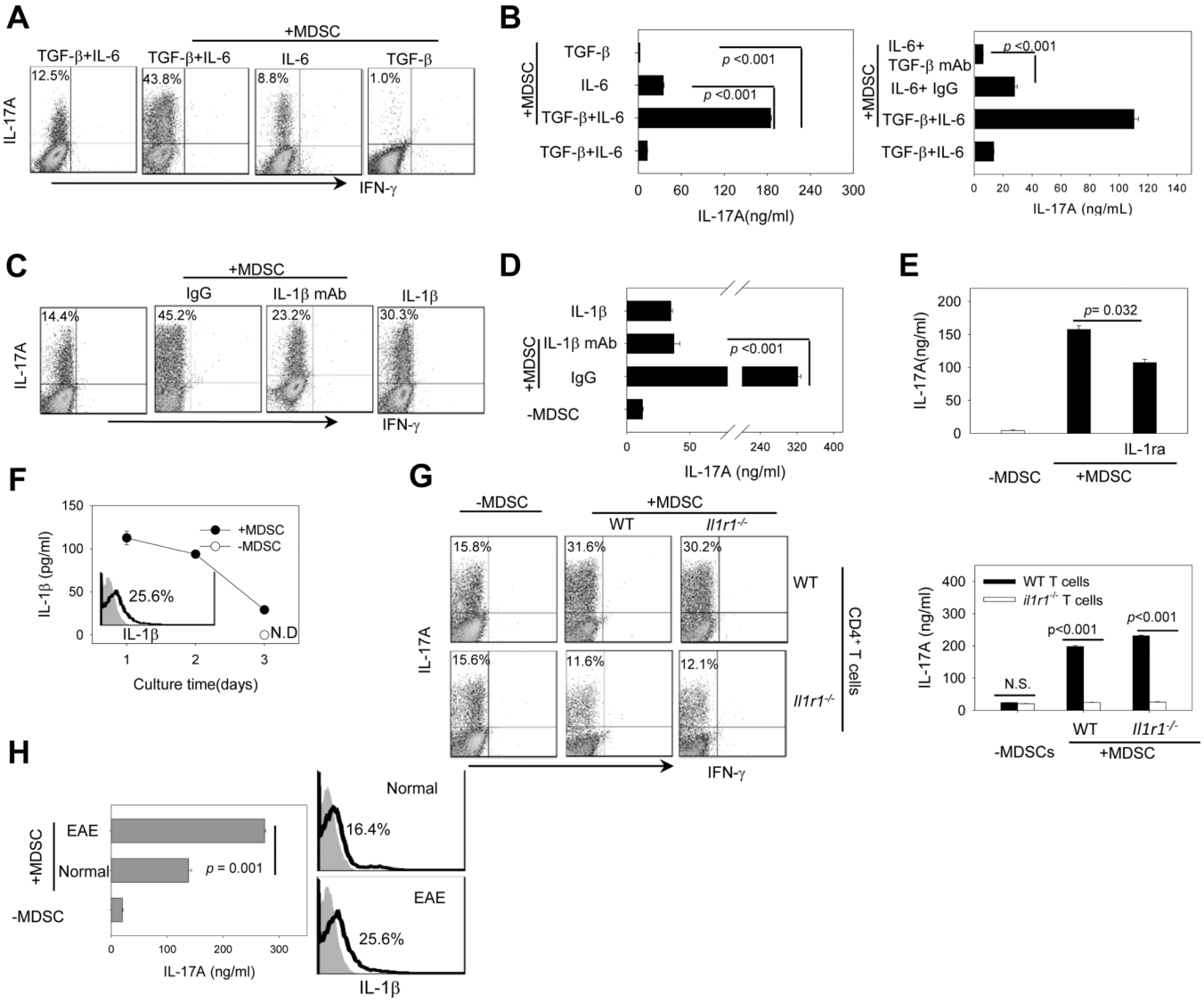

Figure 3. MDSC-enhanced Th17 cell differentiation is mediated by IL-1β

A and **B**. TGF-β or IL-6 are needed for MDSC-stimulated Th17 differentiation. Naïve $CD4^+CD25^-CD62L^+$ T cells were co-cultured with MDSCs under Th17 polarizing conditions in the presence of TGF-β plus IL-6, IL-6, or TGF-β. Intracellular IL-17A staining (**A**) and ELISA assays for IL-17A levels in the culture (**B**, *left*) were performed. Th17 polarization without MDSCs in the culture was used as control. Anti-TGF-β Abs were used to assess the effect of MDSC-derived TGF-β on Th17 polarization (**B**, *right*). **C** and **D**. IL-1β mediates MDSC-enhanced Th17 polarization. Naïve $CD4^+$ T cells were cultured with MDSCs under Th17 polarizing conditions in the presence of IL-1β neutralizing mAb or isotype IgG for 3 days. In one experimental group, IL-1β was added to the culture without MDSCs as a positive control. The percentage of $CD4^+IL\text{-}17^+$ cells (**C**) and IL-17A levels in the supernatant (**D**) were analyzed. **E**. IL-1R antagonist (IL1ra) reduces MDSC-induced IL-17 production. IL-1ra was added to the culture of MDSCs-naïve $CD4^+$ T cells under Th17 polarizing conditions. IL-17A levels were examined by ELISA. **F**. The levels of IL-1β in the Th17 polarizing culture with or without MDSCs were examined by ELISA assays (N.D., not detectable). The intracellular levels of IL-1β in splenic MDSCs from EAE mice were assessed by intracellular staining and flow cytometry analysis (*insert*). Filled gray

indicates isotype control. Solid line indicates IL-1β antibody staining. **G.** IL-1R on T cells is required for MDSC-stimulated Th17 differentiation. Naïve $CD4^+$ T cells from WT or *il1r1*$^{-/-}$ mice were cultured under Th17 polarizing conditions in the presence of MDSCs from WT or *il1r1*$^{-/-}$ mice. Intracellular expression of IL-17A (*left*) and IL-17A levels in supernatant (*right*) were measured by flow cytometry and ELISA. The results shown are from three independent experiments. **H.** Naïve $CD4^+$ T cells were induced for Th17 cell polarization in the presence of MDSCs derived from normal mice or EAE mice. The IL-17A levels in the supernatants were assessed using ELISA assays (*left*). IL-1β expression in MDSCs was examined using intracellular staining assays (*right*). Data represent two independent experiments.

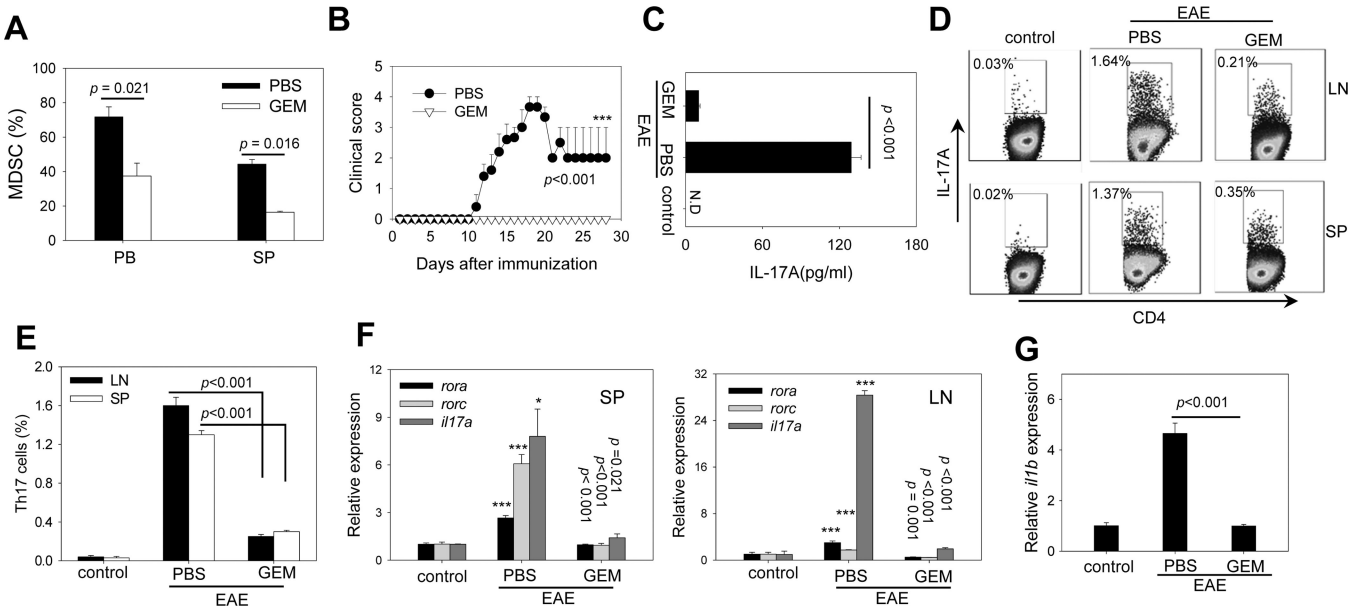

Figure 4. Depletion of MDSCs by GEM reduces the frequency of Th17 cells *in vivo* and ameliorates EAE

A. Efficient depletion of MDSCs by GEM. C57BL/6 mice (n=5) were immunized with $MOG_{35–55}$/CFA on days 0. GEM (100 mg/kg) was administrated i.p. once on day 11. The percentages of $CD11b^{+}Gr\text{-}1^{+}$ cells in peripheral blood and spleen on day 13 (i.e., 2 days after GEM treatment) were examined by flow cytometry. **B**. Blocking of EAE progression by GEM administration. GEM was administrated after EAE induction on days 4, 8, 12, 16. EAE development in mice (n=10) was followed and clinical scores were recorded (***, GEM vs PBS). Data are representative of three independent experiments. **C**. Reduced IL-17A levels in GEM-treated mice. 16 days after MOG immunization IL-17A levels in serum (pooled from 3 mice per group) were measured by ELISA. **D** and **E**. Decreased percentage of Th17 cells in GEM-treated mice. Intracellular in $CD4^{+}IL\text{-}17A^{+}$ T cells in the spleen and draining lymph nodes were examined 23 days after MOG immunization. The numbers indicate the percentages of Th17 cells in $CD4^{+}$ T cells. Bar graph indicating the change in the percentage of Th17 cells before and after GEM treatment is also presented. The results shown represent three independent experiments. **F**. Effect of GEM treatment on *rora, rorc and il17a* gene expression levels in the spleen (*left*) and LNs (*right*). Relative mRNA levels were measured by quantitative real-time RT-PCR and normalized to β-*actin* gene in PBS group (* and ***, PBS vs GEM). **G**. Reduced expression of *il1b* gene in the spleen after GEM treatment. Gene expression of *il1b* was determined by quantitative real-time RT-PCR and normalized to *actin* gene in PBS group. Results shown represent three independent experiments.

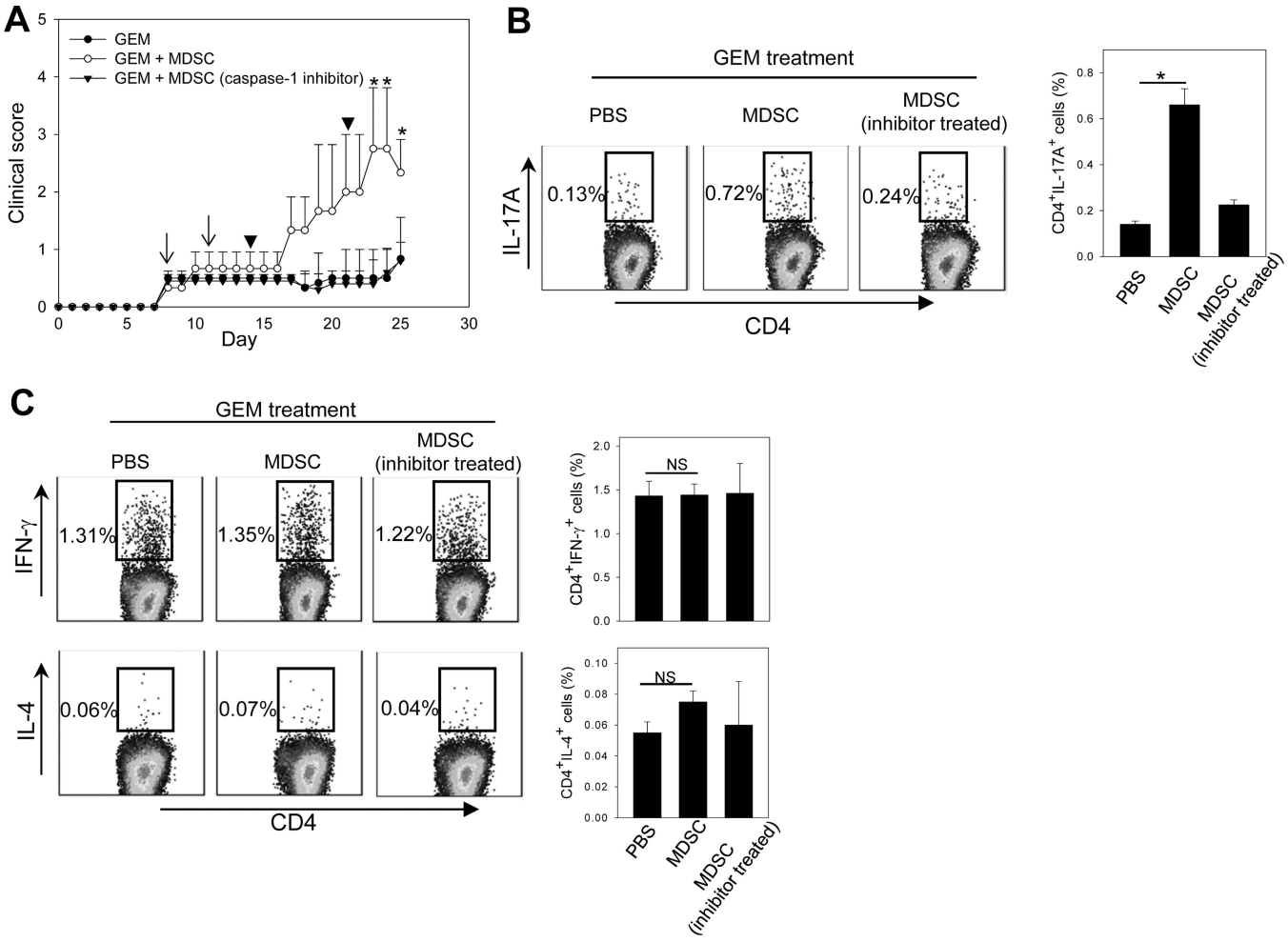

Figure 5. Restoring the EAE disease progression by adoptively transferred MDSCs after GEM treatment is dependent on MDSC-derived IL-1β

A. GEM (50 mg/kg) was administrated to EAE mice twice at 4-day intervals after disease onset (arrows). 4 days after GEM treatment, mice (n=5) received MDSCs or MDSCs pre-treated with the caspse-1 inhibitor twice at one week interval (arrowheads). GEM-treated mice that received PBS served as controls. The progression of EAE disease was followed. *, $p < 0.05$, MDSCs *vs* PBS or inhibitor-treated MDSCs. **B.** The frequency of Th17 cells in the spleen was examined 28 days after MOG immunization intracellular cytokine staining assays. **C.** The presence of Th1 and Th2 cells in the spleen were examined using intracellular staining for IFN-γ or IL-4 in $CD4^+$ T cells, respectively. Bar graphs indicate the changes of Th17, Th1 or Th2 cells before and after MDSC transfer. The results shown represent two independent experiments. *, $p < 0.05$.

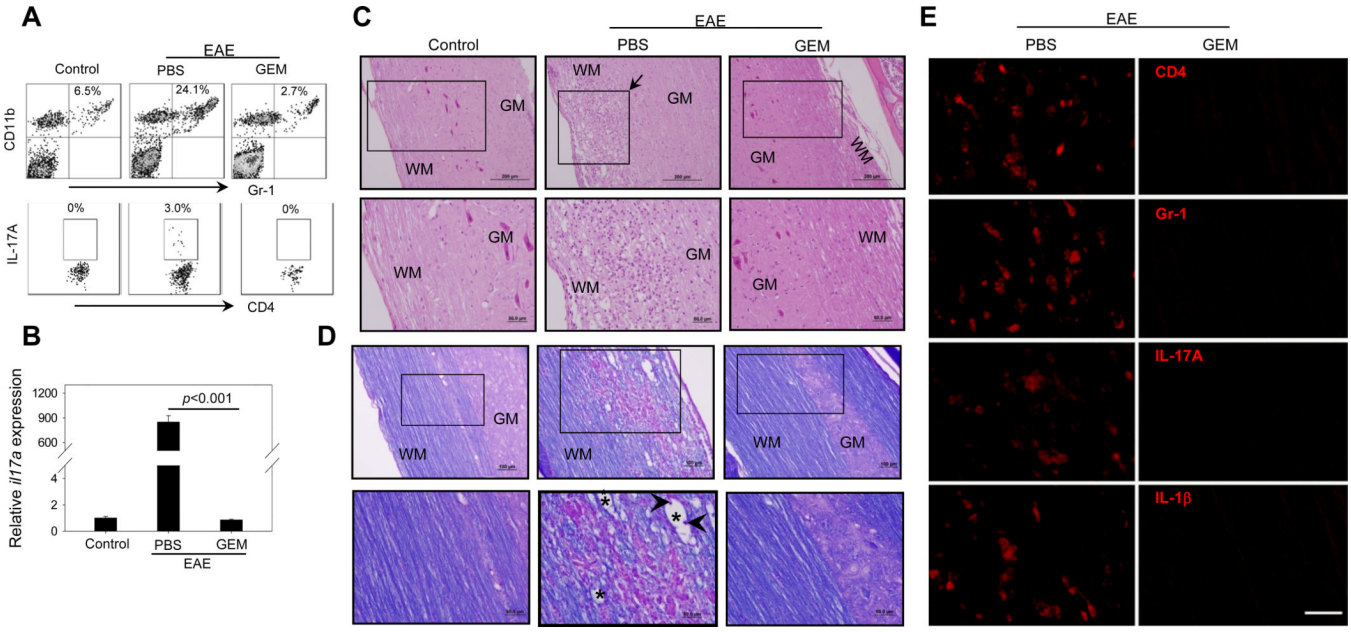

Figure 6. GEM treatment suppresses local inflammation by decreasing Th17 cells and MDSCs in the spinal cords of EAE mice

A. 23 days after MOG immunization, mononuclear cells were isolated from pooled spinal cords of EAE mice (n=3) treated with or without GEM. Cells were subjected to flow cytometry analysis for the presence of $CD11b^+Gr\text{-}1^+$ cells and $CD4^+IL\text{-}17A^+$ cells. The representative histograms from two independent experiments with similar results are shown. **B**. Relative mRNA levels of *il17a* in the spinal cord were examined by real-time RT-PCR. **C** and **D.** Histological analysis of spinal cords from EAE mice with or without GEM treatment. 23 days after MOG immunization, spinal cords were dissected from mice (n=5) and subjected to H&E staining for analysis of parenchymal inflammation (**C**) and Luxol Fast Blue/PAS staining for analysis of demyelination (**D**). WM, white matter; GM, grey matter. The representative cervicothoracic spinal cord sections are shown. Upper panels (100×), scale bar: 100 μm; Lower panels (i.e., high magnification of the boxed area, 200×), scale bar: 50 μm. Arrows in (**C**) indicate inflammatory cell infiltration. Arrowheads and asterisks in (**D**) indicate myelin debris and digestion chamber, respectively. **E.** GEM treatment decreases inflammatory cells and cytokines. Paraffin sections of spinal cords from EAE mice treated with or without GEM were stained with rat anti-mouse mAbs for CD4, Gr-1, IL-17A and IL-1β, followed by incubation with Alexa594-conjugated donkey anti-rat secondary IgG. Staining was examined using fluorescence microscope. Scale bar: 20 μm. Data represent three independent experiments.